JET FORMATION IN PLASMA COMPRESSION IN ACUTE-ANGLE GEOMETRY

V. Ya. Ternovoi

UDC 533.082.5

Shock compression under acute-angle geometry is used with a metallic projectile [1-3] to produce a dense high-temperature plasma. The gas dynamics of the compression may be substantially affected by the interaction between the projectile and the walls of the container at the point of contact. Cumulative jets may be produced from the materials under certain conditions, which may contaminate the gas, produce inhomogeneity in the flow, and reduce the limiting parameters.

Here we analyze the flow conditions as affected by the projector speed w, the semivertex angle of the cone $\alpha/2$, and the material of the projectile and the wall. These factors determine whether a jet is produced from one of the elements (wall or projectile) of both. The discussion is carried out separately for each element, although it is shown that in certain ranges the modes of flow are coupled. An attempt is made to trace the behavior up to very high velocities.

As regards the contact region, we can neglect the differences between conical and planar flows in the initial stage and use results on two-dimensional flows in planar geometry. The theory of jet formation [4] leads us to distinguish subsonic and supersonic velocity regions in the incoming flow in a coordinate system where the point of contact is at rest.

Supersonic Velocity. Figure 1 shows the scheme for the interaction for the jet-free case, which characterizes the velocity pattern in a coordinate system having the point of contact at rest. Then one gets shock waves related to the point of contact. When the flow passes through the oblique shock wave, it may turn without producing a jet only through an angle less than the critical value [5], which is dependent on the properties of the material and the flow speed ($v_1 = w \operatorname{tg} \alpha/2$ for the projectile material and $v_2 = w/\cos \alpha/2$ for the wall material, where w is the projectile speed in the laboratory coordinate system). The actual angle of flow rotation is determined by the direction of the motion in the projectile-wall boundary. The wall material rotates through an angle $\beta/2$ after the point of contact, while the projectile material rotates through $(\pi - \alpha - \beta)/2$. The flow character is determined by comparing these angles with the maximum possible angle of flow rotation.

We subsequently assume that these materials show a linear relation between the shock-wave speed D and the mass velocity discontinuity u [6]:

$$D = a + bu, \tag{1}$$

where $a = a_0 = c_0 = \sqrt{-V_0^2\left(\frac{\partial p}{\partial V}\right)_S}$ is the hydrodynamic velocity under normal conditions for materials not showing phase transitions at small degrees of compression.

The angle of rotation is determined from the condition for equality of the normal components of the velocity vectors for the liner and wall material at the interface and equality of the pressures at that boundary. Simple steps give

$$\operatorname{tg} \beta/2 = \frac{\left(\sqrt{(\rho_2 a_2 + \rho_1 a_1)^2 + 4\rho_1\rho_2 w \sin \alpha/2\,(a_2 b_1 + a_1 b_2 + b_1 b_2 w \sin \alpha/2)} - \right.}{2w\,(\rho_2 b_2 -} \rightarrow$$

$$\rightarrow \frac{\left. - 2\rho_1 b_1 w \sin \alpha/2 - \rho_2 a_2 - \rho_1 a_1\right)}{-\rho_1 b_1)/\cos \alpha/2},$$

where the subscript 1 relates to the projectile parameters and subscript 2 to the wall parameters, while ρ is the density of the material under normal conditions.

Chernogolovka. Translated from Zhurnal Prikladnoi Mekhaniki i Tekhnicheskoi Fiziki, No. 5, pp. 68-73, September-October, 1984. Original article submitted July 4, 1983.

0021-8944/84/2505-0715$08.50

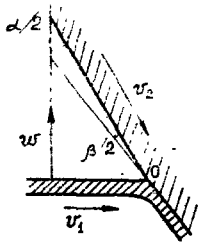

Fig. 1

The angle β/2 increases with the projectile speed and tends to a limit defined by

$$\operatorname{tg}\beta^*/2=\left(\frac{\sqrt{x}}{1+\sqrt{x}}\right)\frac{\sin\alpha}{2},\quad \text{где}\quad x=\frac{\rho_1 b_1}{\rho_2 b_2}.$$

If $\rho_1 b_1 = \rho_2 b_2$, then $(\beta^*/2) = 14°$; the maximum possible angle of rotation for the boundary in the case of an aluminum projectile interacting with a lead wall is 12.3°, while for a molybdenum projectile and a lead wall it is 13.6°.

A solution has been obtained [5] for the supersonic passage of a compressible flow at a rigid wall for a given form for the pressure behind the shock wave $p(\mu)$, where $\mu = \rho/\rho_0 - 1$. In what follows, φ is the acute angle between the shock wave and the rigid wall, while θ is the angle between the initial direction of motion of the flow and the rigid wall.

From (1) we get the following expression for the pressure behind the shock wave:

$$p=\frac{\rho_0 a^2\mu(\mu+1)}{(1-b\mu+\mu)^3}.$$

On repeating the expressions, following [5], we get a system of equations for the maximum angle of rotation without jet formation:

$$\mu=\begin{cases}\dfrac{(b-1)M^2+b/2+1\pm\sqrt{b(M^2(2b-1)+1+b/4)}}{(b-1)^2M^2-1} & \text{for}\quad M\neq(b-1)^{-1},\\ \dfrac{M^2-1}{2(1+b/2+(b-1)M^2)} & \text{for}\quad M=(b-1)^{-1};\end{cases}\tag{2}$$

$$\sin\varphi=\frac{(1+\mu)}{(1-(b-1)\mu)M};\tag{3}$$

$$\operatorname{tg}\theta^*=\frac{\mu\sqrt{1-\sin^2\varphi}\sin\varphi}{1+\mu-\mu\sin^2\varphi},\tag{4}$$

where $M = v/a$ and v is the speed of the incident flow. From the condition that v tends to zero as the flow speed decreases, we take the minus sign in front of the root in (2). This solution enables one to find the asymptote as the velocity increases, in contrast to [7]:

$$\mu\to\frac{1}{(b-1)}-\frac{\sqrt{b(2b-1)}}{(b-1)^2M},$$

$$\sin\varphi\to\sqrt{\frac{b}{(2b-1)}}-\frac{1}{M(b-1)},\quad \operatorname{tg}\theta^*(\infty)=\frac{1}{2\sqrt{(b-1)b}}.$$

In the limit of high velocities, there is a maximum angle of rotation which is dependent only on parameter b in the equation relating D and u. The maximum angle is 30° for b = 1.5, as against 42.5° for b = 1.24 and 41° for b = 1.26 (the limiting value of b for metals was found from the Thomas-Fermi model as 1.25 [6]). In [8], it was shown from theory and experiment that the jet formed in a supersonic flow is dispersed, and the density of the cloud of particles is the less the less the angle of rotation differs from the maximum possible angle for jet-free flow. It was also shown there that when the flow speed is approximately equal to the speed of sound, there is a slight radial dispersal of the jet; if the flow speed is subsonic, one gets continuous connecting jets.

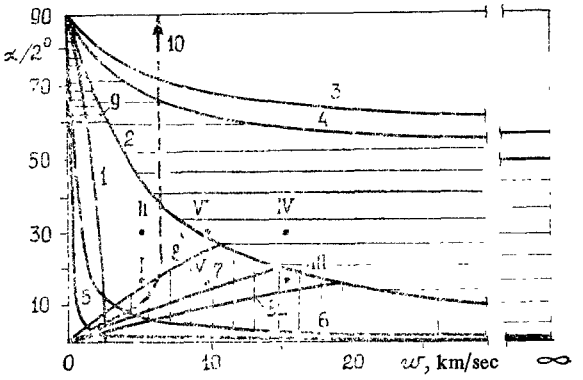

Fig. 2

Subsonic Velocity. In the subsonic region of flow for the material in the area of the contact, it is usual to base the argument on an ideal incompressible-fluid model. The hydrodynamic theory of cumulation always predicts a cumulative jet for any collision geometry [4]. As a metal has strength parameters [9] and viscosity [10], a jet is not formed under subsonic conditions with certain collision parameter.

When the strength of the materials is incorporated, there is no jet formation at low incident flow speeds:

$$w_1^{0*} = \sqrt{\frac{2\sigma_1}{\rho_1}}\frac{1}{\sin\alpha/2}, \quad w_2^{0*} = \sqrt{\frac{2\sigma_2}{\rho_2}}\frac{1}{\operatorname{tg}\alpha/2} \tag{5}$$

(σ is strength). In [9], examples are given of the strength: σ = 0.4-0.5 GPa for steel and σ = 0.2-0.3 GPa for aluminum. The experiments discussed below show that this constraint is unimportant.

The incompressible viscous liquid model has been used [10] to explain the occurrence of retarded jets and the absence of jets in a velocity range dependent on the geometrical dimensions of the interacting flows. The maximum flow speed sllowing of jet-free interaction is defined as

$$w_1^{1*} = 2\left(\frac{1-\cos\alpha/2}{\cos^2\alpha/2}\right)\frac{\nu_1}{\delta}\frac{1}{\operatorname{tg}\alpha/2}, \quad w_2^{1*} = w_1^{1*}\frac{\nu_2}{\nu_1} \tag{6}$$

where ν is the kinematic viscosity, δ is the thickness of the interaction region, and $(\pi - \alpha)/2$ is the collision angle. It was shown also in [10] that the viscosity tends to limiting values of 10^4-10^5 P as the deformation rate increases. Values are given in [11] for the viscosities of particular metals in the strain rate range of interest here.

A jet is formed in the rest of the region of collision parameters. Most experiments confirm the suggestion [8] that the jet is compact. However, at small collision angles (larger than $\alpha/2$), the jets are dispersed, as in the supersonic state. This is due to instability in the interface between the colliding flows [12]. This region corresponds to the region of explosive welding modes and covers collision angles less than 60° ($\alpha/2 > 60°$).

This analysis shows that the plane in coordinate w and $\alpha/2$ is divided up into the regions shown in Fig. 2, where 1 and 2 are lines on which the speeds of the wall and projectile material attain their sonic values, while line 3 corresponds to $\alpha/2 = (\pi/2 - \theta^*(M))$ for the projectile material and line 4 with $(\alpha/2) = (\pi/2 - \theta^*(M) - \beta/2\,(M))$ represents the limit of jet-free supersonic states when allowance is made for the wall compressibility. Figure 2 shows the case where the maximum angle of rotation in the wall material is always greater than the angle of rotation of the interface beyond the contact point. The boundaries 5 and 6 are defined by w_1^{0*}, w_2^{0*} from (6) for the wall and projectile materials correspondingly: lines 7, 8, and 8_ show correspondingly w_1^{1*}, w_2^{1*} for particular cases (boundary 8_ has been drawn for the use of a projectile thinner than for 8 and an unchanged value of ν). Line 9 ($\alpha/2$ = 60°) separates the regions of continuous and dispersed jets at subsonic flow speeds. Boundaries 2 and 4 distinguish the region of dispersed jets at supersonic flow speeds: 2, 8, 7 or 8_ and 6 denote the region of continuous jets. The Roman numerals in Fig. 2 denote

TABLE 1

No.	I	II	III	IV	V	VI
Projectile material	Aluminum				Molybdenum	
Wall material	Lead					
Projectile thickness, mm	0,2	0,2	0,03	0,03	0,1	0,1
$\alpha/2$, deg	15	30	15	30	15	30
w, km/sec	5,4	5,4	15	15	9,3	9,3
v_1, km/sec	1,45	3,1	4,0	8,65	2,5	5,35
v_2, km/sec	5,6	6,2	15,5	17,3	9,6	10,7
$\beta/2$, deg	6	8	5	8	8	13
θ_1^*, deg				7		1
θ_2^*, deg	13	15	28	29	22	24
w_1^{0*}, km/sec	1,8	0,9	1,8	0,9	2,4	1,25
w_2^{0*}, km/sec	0,3	0,15	0,3	0,15	0,3	0,15
w_1^{1*}, km/sec	35	81	230	530	110	250
w_2^{1*}, km/sec	6,2	14	41	94	12	29

the positions of the flow modes in particular conical targets. The scheme for recording the parameters of the hot dense plasma has been given in [13] and so is not considered here.

Table 1 gives the parameters and the results obtained under the above scheme. We give results for systems where layered materials were used as well as those for constructions where thicker projectiles are used to generate plasma [13]. The layered system consisted of a steel projectile accelerated to a speed of 5.3 ± 0.2 km/sec, Lucite insert of thickness about 1 mm, and a molybdenum foil of thickness 0.1 mm, which was accelerated by the projectile to a speed of 9.3 ± 0.5 km/sec and which interacted with the aluminum bottom of the target of thickness 0.03 mm.

We used the equations of state for lead, molybdenum, and aluminum with the parameters given in Table 2. Table 2 also gives the characteristic values for the strength and kinematic viscosity for each of these metals.

In all these cases, the wall material had a supersonic flow speed v_2. A dispersed jet was not formed, since $\beta/2$ was less than the maximum possible angle of rotation without jet formation θ_2^*.

It is evident that these systems, apart from the high-speed one with $\alpha/2 = 30°$, fall in the region of subsonic flow speed for the projectile material v_1 at the point of contact.

On incorporating the strength parameters via (5), one gets low limiting velocities for the projectile (w_1^{0*}) and the wall material (w_2^{0*}) in jet-free flows, and there is no constraint on the jet formation in such systems. The viscous forces hinder jet formation; w_1^{1*} and w_2^{1*} are the limiting velocities of the projectile for jet-free flow of the projectile and wall materials correspondingly when one incorporates the viscous forces in accordance with (6). It is evident that these velocities greatly exceed the velocity range actually realized in these systems.

TABLE 2

Material	$\rho \cdot 10^{-3}$, kg/m^3	a, km/sec	b	ν, m^2/sec	σ, GPa
Lead	11,34	2,58	1,26	4,6	0,04
Molybdenum	10,2	5,16	1,24	40	2,0
Aluminum	2,71	5,25	1,39	26	0,3

The value of ν was taken from [11], while the value of δ was equal to the projectile thickness. One can increase w_1^1* and w_2^1* for a given angle by reducing the projectile thickness and obtain jet-free states over much of the region bounded by line 2 (Fig. 2). It is important that the evaluation has been performed with unaltered values of ν, although the viscosity may be dependent on the deformation conditions. However, it is impossible to incorporate this dependence at present because of the lack of experimental data. On the other hand, the jets will be compact under subsonic conditions (large angles of collision). Supersonic conditions will result in dispersed jets. This is evidently the reason for the marked reduction in the plasma parameters recorded by the method of [13] by the use of targets with $\alpha/2 = 30°$ and high projectile speeds. The analysis of the maximum angles of rotation without jet formation shows that for $\alpha/2 < 30°$ with the materials used, one cannot hope to produce a jet-free flow as the projectile velocity steadily increases because $\theta^*(\infty) + \beta^*/2(\infty) < (\pi - \alpha)/2$. Jet-free configurations are possible for large semivertex angles in the cone. This parameter range is suitable for plasma compression with the use of generators similar to the Voitenko generator. Figure 2 shows that jet-flow regions occur in a hemispherical compressor chamber (line 10); a larger amount of metal may enter the compressed plasma on account of the jet formation, along with the action of the plasma on the chamber wall [4].

Therefore, analytic expressions have been obtained for the critical angle of rotation in a compressible supersonic flow having an equation of state employing a linear relation between the shock-wave speed and the step in the mass velocity. The asymptotes to the solutions have been found for the critical angle of rotation and the angle of rotation of the interface as the projectile speed increases. It is shown to be important to incorporate jet formation in designing devices for plasma compression under acute-angle geometry conditions.

I am indebted to V. E. Fortov for formulating the problem and for constant interest, and to V. B. Mintsev, A. N. Mikhailov, and A. V. Utkin for useful discussions.

LITERATURE CITED

1. S. I. Anisimov, V. I. Vovchenko, et al., "A study of the generation of thermonuclear neutrons in laser action on conical targets," Pis'ma Zh. Tekh. Fiz., 4, No. 7 (1978).
2. H. Derentowies, S. Kaliski, J. Wolski, and Z. Ziolkowski, "Generation of thermonuclear fusion neutrons by means of a pure explosion. 2. Experimental results," Bull. Acad. Polon. Sci., 25, No. 10 (1977).
3. A. E. Voitenko, "Production of high-speed gas jets," Dokl. Akad. Nauk SSSR, 158, No. 6 (1964).
4. S. A. Kinelovskii and Yu. A. Trishin, "Physical aspects of cumulation," Fiz. Goreniya Vzryva, 16, No. 5 (1980).
5. J. M. Walsh, R. G. Shleffler, and F. J. Willing, "Limiting conditions for jet formation in high velocity collisions," J. Appl. Phys., 24, No. 3 (1953).
6. L. V. Al'tshuler, A. A. Bakanova, et al., "Shock adiabats for metals: new data, statistical analysis, and general regularities," Zh. Prikl. Mekh. Tekh. Fiz., No. 2 (1981).
7. G. E. Kuz'min and I. V. Yakovlev, "A study of collisions between metallic plates with supersonic velocities at the point of contact," Fiz. Goreniya Vzryva, 9, No. 5 (1973).
8. P. C. Chou, J. Carleone, and R. R. Karpp, "Criteria for jet formation from impinging shells and plates," J. Appl. Phys., 47, No. 7 (1976).
9. A. A. Deribas and I. D. Zakharenko, "Determining the limiting collision conditions providing explosive metal welding," Fiz. Goreniya Vzryva, 11, No. 1 (1975).
10. A. K. Godunov, A. A. Deribas, and V. I. Mali, "The effects of viscosity on jet formation in the collision of metallic plates," Fiz. Goreniya Vzryva, 11, No. 1 (1975).
11. A. A. Deribas, Physics of Explosive Hardening and Welding [in Russian], Nauka, Novosibirsk (1980).

12. A. N. Mikhailov, A. N. Dremin, Yu. A. Gordopolov, and A. V. Utkin, "Wave formation at a collision boundary between metals as the reason for reverse-jet decomposition," in: International Symposium on Explosive Metalworking [in Russian], Gottvaldov, Czechoslovakia (1982).
13. S. I. Anisimov, V. E. Bespalov, et al., "Neutron generation in explosive initiation of the DD reaction in a conical target," Pis'ma Zh. Eksp. Teor. Fiz., 31, No. 1 (1980).
14. V. B. Mintsev and V. E. Fortov, "Explosive shock tubes," Teplofiz. Vys. Temp., 20, No. 4 (1982).

PHOTOCHROMIC METHOD OF VISUALIZING HYDRODYNAMIC FLOWS

V. A. Barachevskii, V. F. Mandzhikov, Yu. S. Ryazantsev,
Yu. P. Strokach, and V. N. Yurechko

UDC 532.574.8

The traditional methods of visualizing flow in a liquid involve introducing tracers, colored liquid, solid particles, or bubbles [1, 2].

The photochromic method involves the use of colored markers initiated by UV irradiation in the initially colorless liquid, in which the photochromic substance is dissolved [3]. As the photo-induced color persists for a certain time, it is possible to record the color label visually or by means of a camera [4].

The photochromic method is a noncontacting one, and it introduces virtually no perturbations into the flow, and thus can provide repeated fast production of colored lines, intersecting lines, and planes at a given point within the flow by the use of collimated UV radiation.

The photochromic method was proposed in 1967 and was developed in [5-11]. The method has been used to examine turbulence in circular tubes, to determine the velocity pattern in flow around a sphere, and to examine the flow at the wall in a rough tube [7-11]. The photochromic compounds are mainly derivatives of dinitrobenzylpyridine, which are dissolved in alcohol or kerosene, and the lengths of the colored labels do not exceed 2.5 cm, which substantially restricted the utility of the method. We have used compounds from the class of nitro derivatives of indoline spiropyrans SPP, which produce labels of various colors in accordance with the nature of the SPP and the solvent [3]. The SPP powder was dissolved in distilled water, alcohol, or silicone oil. The photochromic reaction produced by UV radiation involves a reversible transition from the colorless state to the colored one as follows:

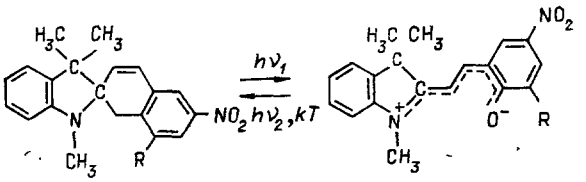

One can adjust the color and the lifetime of the colored form by introducing substituents with various donor-acceptor features in position R.

The experiments were performed with the apparatus shown schematically in Fig. 1, where 1 is an FS-7 filter, 2 are lenses, 3 is a ZhZS-9 filter, 4 is the hydraulic channel, 5 a matt screen, and 6 a KV-1000 cine light. The colored mark was produced by the radiation at the second harmonic of a ruby laser, λ_1 = 347 nm. The Q-switched single-pulse ruby laser type OGM-20 was used as the master oscillator, with subsequent amplification in a single-phase amplifying stage type GUS-1 [12]. To transform the basic ruby radiation λ_0 = 649 nm into the second harmonic with λ_1 = 347 nm, we used a KDP nonlinear component [12]. The energy in the fundamental after amplification was 2-3 J. Also, 2-3% of the fundamental was converted to the second harmonic.

Moscow. Translated from Zhurnal Prikladnoi Mekhaniki i Tekhnicheskoi Fiziki, No. 3, pp. 73-76, September-October, 1984. Original article submitted July 13, 1983.

 0021-8944/84/2505-0720$08.50